

¹H NMR Characterization of Swelling in Cross-Linked Polymer Systems

P. J. O'Connor,[†] S. S. Cutié,[†] P. B. Smith,^{*,†} S. J. Martin,[‡] R. L. Sammler,[§] W. I. Harris,[⊥] M. J. Marks,^{||} and L. Wilson[¶]

Analytical Sciences Laboratory, Advanced Materials, Materials R&D Laboratory, and Liquid Separations Research, The Dow Chemical Company, Midland, Michigan 48667, Texas Polymer Center, The Dow Chemical Company, Freeport, Texas 77541, and Superabsorbent Products R&D, The Dow Chemical Company, Midland, Michigan 48674

Received May 2, 1996; Revised Manuscript Received September 3, 1996[®]

ABSTRACT: A ¹H NMR method capable of determining the level of swelling of microscopic volume elements (about 20 μm in diameter) within cross-linked materials is described. The fact that it is a microscopic swell measurement makes it extremely useful for the characterization of the swelling heterogeneities which may exist within common network systems, such as core/shell or other morphologies. The method utilizes the differences in chemical shift between solvent absorbed into the cross-linked polymer and that of solvent outside the polymer. This chemical shift difference is then correlated to macroscopic swelling (rather than cross-linking) through a simple model which encompasses both the effective chemical cross-links and the entanglement cross-links in the manner of classical swelling experiments. The analysis is demonstrated for styrene, divinylbenzene copolymer beads, cross-linked polycarbonates, ion-exchange cation resins and cross-linked poly(acrylic acid). A calibration is, in each case, developed with a series of standard materials whose bulk swelling characteristics were determined. An example of the analysis of the cross-linking morphology within a single cation-exchange bead is also presented. The analysis of swelling by this ¹H NMR method appears to be applicable to any network system with aromatic or acid functionality. Its application is expected to enable identification of new structure/property relationships critical for developing advanced materials.

Introduction

Cross-linked polymers are found in many and varied applications throughout the chemical industry including rubbers, latexes, urethanes, epoxies, aqueous fluid absorbers, and ion-exchange resins. The level and distribution of cross-linking in cured networks has been very difficult to characterize in these systems spectroscopically because even low levels of cross-linking often render the material intractable. Cross-linking levels in rubbery materials are often measured with equilibrium modulus experiments or swelling experiments.¹⁻⁴ Both experiments provide key metrics often well correlated to resin physical properties. These correlations are attributed to proper weighting of chemical and entanglement cross-links (or equivalently the effective network chains). Both experiments are commonly applied to provide estimates of mean cross-linking levels, and their results are best suited for uniform samples. Nevertheless, many materials with nonuniform cross-link levels are utilized in applications for which their performance is linked undoubtedly to this nonuniform structure. Therefore, its characterization is key to finding new structure/property relationships critical for developing advanced materials.

The NMR methodology described here is a swelling experiment which is capable of probing the cross-link heterogeneity in domain sizes as small as 20 μm. Samples may be composed of many small particles (>0.1 mm) or of single particles as large as several millimeters

in diameter. The sample heterogeneity may arise from internal structure within each particle, a blend of different uniformly cross-linked particles, or local domains within a rubbery solid. The study of particles with spherical symmetry offers several advantages which will be discussed subsequently, and therefore, much of this study focuses on a set of uniformly cross-linked spherical beads of poly(styrene-*co*-divinylbenzene) resins and their sulfonated counterparts, which possess submillimeter diameters. Key to these studies is the measurement of solvent chemical shifts for slurries of solvent-swollen beads, and establishing a relationship between the NMR data and classical swelling measurements for a set of spatially-uniform cross-linked standards made with divinylbenzene levels below 25 wt %.

These NMR experiments, which focus on the solvent rather than the network chains, are expected to weight cross-links in a manner similar to classical swelling experiments, and consequently be critical to understanding the resin physical properties. Multiple solvent resonances in the spectra of the slurry of swollen beads, when observed, are expected to fingerprint the sample cross-linking heterogeneity.

Several other NMR techniques have been used for cross-linking studies of ion-exchange resins and their unfunctionalized poly(styrene-*co*-divinylbenzene) precursors. Many techniques focus on the resin chain dynamics. These molecular probes, such as the ¹³C NMR line width and relaxation studies of swollen poly(styrene-*co*-divinylbenzene),^{5-13,23,24} provide new and complementary information about the cross-linking levels in heterogeneous samples but are difficult to quantify. They may also not be readily related to the resin physical properties in that they are expected to weight chemical and entanglement cross-links differently than those of classical modulus and swelling experiments.

* To whom correspondence should be addressed.

[†] Analytical Sciences Laboratory.

[‡] Advanced Materials.

[§] Materials R&D Laboratory.

[⊥] Liquid Separations Research.

^{||} Texas Polymer Center.

[¶] Superabsorbent Products R&D.

[®] Abstract published in *Advance ACS Abstracts*, October 15, 1996.

Solid state NMR was also utilized but the level of cross-linking did not change the density of the copolymer in the nonswollen state, and therefore, this method was not sensitive to the level of cross-linking. High-resolution ^1H NMR for the characterization of cation-exchange resins was described as early as the early 1970s.^{14–22,25} In these experiments two lines are observed for water-swollen cation-exchange resins (sulfonated S–DVB copolymers). One of the lines was due to water outside the bead and the other due to water inside. The origin of the shifts was due to the pH effects. Since the pores of the cation beads were acidic, the absorbed water was shifted downfield from that of the external water line.²⁶ This method gave a very precise determination of the swelling of the beads and was actually used in the analysis of single beads. Therefore, the distribution of swelling due to intrabead cross-linking distributions could be differentiated from interbead distributions.

A recent publication described the use of chloroform as a probe molecule for the ^1H NMR method for the analysis of the cross-linking distributions within S–DVB copolymers.²⁷ The shift for the absorbed chloroform was upfield from the interstitial chloroform due to susceptibility effects. The chemical shift of the chloroform was shown to be a function of the level of DVB in the copolymer.

This work presents three significant new ideas in this field. First, it demonstrates that the ^1H NMR chemical shifts are primarily dependent on the macroscopic swelling, not cross-linking. This is a subtle but important distinction because swelling encompasses the chemical cross-links, the entanglement cross-links, and the molecular weight of the primary chain.¹ Second, this work quantifies the effects observed for the chloroform probe method using a set of well-characterized S–DVB copolymer standards ranging from 0.1 to 25 wt % divinylbenzene and sulfonated cation resins made from these S–DVB copolymer precursors. Special effort was taken to ensure that the standards were all made under similar conditions and could, therefore, be used to develop a calibration of the NMR shifts to copolymer swelling. Third, the method is shown to have broad application to network polymers which possess aromatic or acidic functionality, using a cross-linked polycarbonate system and cross-linked poly(acrylic acid) superabsorbents as examples. Magic angle spinning (MAS) ^1H NMR techniques were employed for the analysis of single beads of cation-exchange resins with internal cross-linking morphology and for samples of nonspherical shape.

Experimental Section

Synthesis. Fifteen cross-linked resins of poly(styrene-co-divinylbenzene) were made with weight fractions w_{DVB} of divinylbenzene ranging from 0.02 to 0.25. (The weight fractions of DVB quoted are based on active DVB even though 55% DVB was used in the recipe.) The synthesis of these random copolymers employed a batch free-radical suspension polymerization in a 2.5 L reactor. The reactor was charged with the monomers (styrene and 55% divinylbenzene; 1200 g total), a free-radical initiator (0.0052 mol), deionized water (700 g), and a cellulosic suspending agent (1% active in water, 100 g). The air in the reactor was purged with nitrogen, and the reactor was sealed and stirred with a Anchor-type agitator at 240 revolutions/min. The polymerization was conducted at 75 °C for 10 or 12 h, and later

Table 1. Properties of the Cation-Exchange Resins

weight % DVB	% water retention capacity at RT	dry weight capacity (mequiv/g of resin)	wet volume capacity (mequiv/mL)
2.0	77.7	5.53	0.91
3.0	70.4	5.39	1.18
4.0	66.0	5.23	1.28
5.0	60.2	5.27	1.70
5.9	55.7	5.03	1.83
7.3	53.7	5.35	2.02
7.9	52.1	5.25	2.07
8.9	49.5	5.28	2.12
9.8	47.6	5.20	2.26
11.9	43.3	5.27	2.47

elevated to 110 °C for 3 h. This polymerization transforms the monomer into a slurry of spherical beads with submillimeter diameters. After cooling to room temperature, the slurry was filtered and washed with deionized water. The colorless beads were air dried and screened to remove a few large irregular-shape particles. The other samples of this study were made similarly but with different size reactors. The particle size distribution of the beads was typically a Rosin–Rammler distribution between about 0.05 and 1 mm, centered at about 0.5 mm.

Characterization of the extent-of-reaction and the glass transition temperatures of many of these samples have been reported elsewhere.³² The sol fractions were expected to be small for these free-radical polymerization beads and were not extracted prior to the swelling experiments.

The beads were converted to cation-exchange resins using the following conditions. The beads were swollen with methylene chloride and sulfonated using concentrated sulfuric acid at 120 °C for 2 h. The ratio of resin to sulfuric acid and methylene chloride was at least 1/6/0.5. The samples were then washed with deionized water for 300 min at 70 °C. Sulfonation, when complete, should ideally introduce one sulfonate group to each aromatic ring in the copolymer precursor and have no effect on the cross-linking levels. However, some cross-links may be formed by sulfone formation while other cross-links may be degraded by the sulfonation process.

Several properties of the cation-exchange resins are summarized in Table 1. The water retention capacities were measured by centrifugation at room temperature and drying at elevated temperature in a moisture balance. Dry weight and wet volume capacities were measured by titration. The properties were typical of those found for batch resins. The higher cross-linked copolymers (>14% DVB) were very difficult to sulfonate, as indicated by their dry weight capacities. Their sulfonations were abandoned after several attempts and, consequently, cross-linking standards are limited to DVB levels less than 14% for the cation-exchange resins.

Cross-Linked Poly(acrylic acid). The samples were prepared by the water in oil (w/o) suspension polymerization of 25 wt % solids aqueous solutions of sodium acrylate in kerosene. The recipe used for each sample is given in Table 2. The aqueous phase was prepared by adding acrylic acid (Rohm and Haas, flocculant grade) to deionized water. The bis(acrylamido)acetic acid cross-linker (Polysciences), whose structure is given below, was then added followed by diethylenetriaminepentaacetic acid chelant (VERSENEX*-80, Dow Chemical). The VERSENEX*-80 prevented premature polymerization initiated by adventitious metals. The solution was then slowly neutralized with

Table 2. Polymerization Recipes for Poly(acrylic acid) Samples

	sample		
	69-93B	69-93C	69-97A
mole fraction cross-linker	0.0005	0.00503	0.0526
weight of acrylic acid (g)	99.86	98.63	86.75
weight of DI water (g)	184.22	185.09	193.48
weight of bAmAA (g) ^a	0.1374	1.3699	13.2350
weight of 10% V-80 (g)	4.00	4.00	4.00
weight of 50% NaOH (g) ^b	110.92	110.05	101.66
weight of 5.8% persulfate (g)	0.86	0.86	0.86

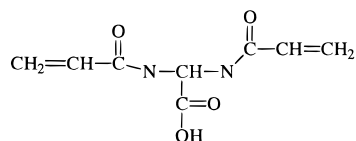
^a Bis(acrylamido)acetic acid. ^b Results are given for complete neutralization of acrylic acid and cross-linker.

50 wt % sodium hydroxide in water (Fisher certified grade), with cooling provided by an ice bath. The sodium persulfate (Aldrich 98+%) was then added as a 5.8 wt % solution in DI water. This corresponded to 500 ppm based on monomers in the acid form. This procedure yielded 400 g of aqueous phase.

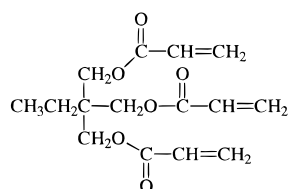
The continuous (oil) phase was prepared by dispersing 0.58 g of Aerosil* R972 hydrophobic fumed silica (Degussa) into 400 g of Isopar* L deodorized kerosene (Exxon) using a commercial blender. This was combined with an additional 400 g of ISOPAR L in a jacketed 2 L resin kettle. To this was added 0.86 mL of trimethylolpropane triacrylate (TMPTA, Sartomer), whose structure is given below, to suppress agglomeration. Only a negligible amount of this cross-linker partitioned into the aqueous phase at the solids and neutralization employed. Agitation was provided by an impeller system rotating at 250 rpm. The aqueous phase was added and the vessel was sparged with nitrogen for 40 min at a flow rate of 750 mL of STP/min to deoxygenate. This combination of suspension system and agitation yielded an average particle size of 400 μm .

After the deoxygenation and sizing, the jacket was connected to a 60 °C recirculating water bath to thermally initiate the polymerization. The temperature of the reactor contents peaked at 75 °C after 13 min, and the water bath was held at 60 °C for an additional 1 h. The reactor was then cooled, and the product beads were filtered off and dried in a forced-air explosion-proof oven at 100 °C overnight. The suspension system left a hydrophobic surface on the product. To counteract this effect, 0.25 wt % VORANOL* 2070 ether polyol (Dow) was dripped onto the product with slight mixing.

The samples were converted to the acid form by placing beads in a column and swelling and eluting with five column volumes of 0.1 M HCl.



Bisacrylamido acetic acid



Trimethylolpropane Triacrylate

Cross-Linked Polycarbonate. The cross-linked Bisphenol A polycarbonate samples (BCB-PC) were

made with benzocyclobutene (BCB) end groups using 4-hydroxybenzocyclobutene (BCB-OH).³⁵ The molecular weights were controlled by varying the mole ratio of BCB-OH to Bisphenol A (termed mole/mole or m/m). Due to the functionality of the BCB once these terminal groups are reacted with applied heat, the molecular weight between cross-links, M_c , of the cross-linked BCB PC's is about $1.6M_n$ measured before the cure above 200 °C. Thereby, a system of controlled cross-link density was produced. The samples were compression-molded films of about 1 mm thickness having no measurable soluble fraction. They were swollen for 2 days prior to the analysis.

Volume Expansions. An empty 50-mL graduated cylinder was charged with 10 mL of beads of poly(styrene-*co*-divinylbenzene) treated with antistat. The cylinder was vibrated to promote settling. The copolymer volume in its unswollen state V_0 was 10 mL. About 50 mL of solvent was poured into the cylinder, and the cylinder was closed with a ground-glass stopper. The copolymer was allowed to swell to its time-independent state at room temperature (near 25 °C). The copolymer expanded volume was recorded as V_e . About 24 h was required for the swelling of copolymer with w_{DVB} below about 0.09; 5 days was used for the higher- w_{DVB} copolymers. The volume expansion is given by $V_e/V_0 - 1$. The copolymers floated in chloroform and sank in toluene.

NMR. The polymers were swollen in HPLC grade chloroform and allowed to equilibrate for a minimum of 1 day before analysis by ¹H NMR spectroscopy. After 1 day of swelling, no further change in the relative shift was observed. Analyses were performed by transferring a volume of the copolymer-bead chloroform slurry into a 5 mm NMR tube. The ¹H NMR spectra were obtained at 300 MHz using a Bruker AC-300 NMR spectrometer, model number HO2129-ECL-24, S/N 0898. The typical data acquisition parameters utilized were as follows: pulse width = 90°, delay time = 10 s, size = 16K, accumulation time = 0.41 s, sweep width = 20 kHz, apodization = exponential, 1 Hz broadening. The probe temperature was thermostated at 303 K unless stated otherwise. The absolute resonance of chloroform external to the beads (i.e. nonabsorbed) was assigned a value of 7.24 ppm. The chloroform ¹H spin-spin relaxation times (T_2) were measured using the Carr-Purcell-Meiboom-Gill (CPMG) sequence.²⁹ Spin-lattice relaxation times (T_1) were calculated using a three parameter fit equation with SIMFIT version 880601.1 on the Bruker data system. High-field NMR measurements were performed on a General Electric Omega 600 instrument with a nominal operating frequency of 600 MHz.

Magic angle spinning (MAS) ¹H NMR analysis was performed at 200 MHz using a Bruker MSL-200 spectrometer. Spectra were acquired at ambient temperature (about 23 °C) with exponential apodization. The data acquisition parameters utilized were as follows: pulse width = 60° (4 μ), delay time = 5 s, size = 4K, accumulation time = 0.80 s, sweep width = 10 kHz, apodization = exponential, 1.0 Hz broadening. Spinning rates ranged from 1.1 to 1.8 kHz.

Results

Theoretical Basis. S-DVB Copolymers Swollen with Chloroform. The ¹H NMR methodology used is a microscopic swell measurement. The NMR signal of the solvent absorbed into the copolymer bead depends

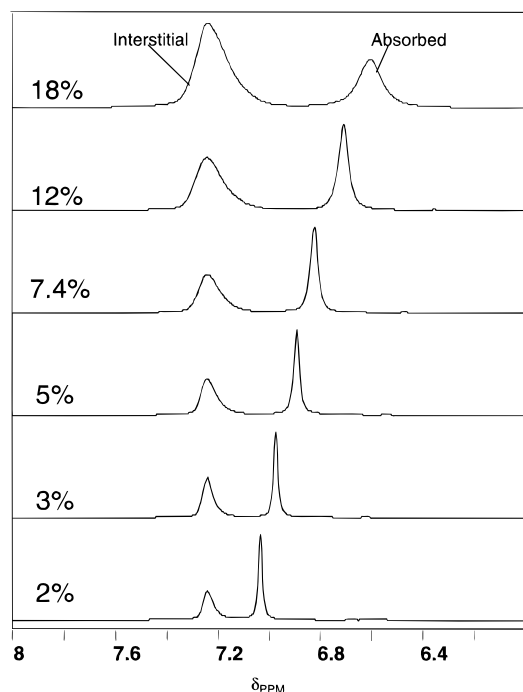


Figure 1. Dependence of the ^1H NMR spectrum of chloroform absorbed in styrene-divinylbenzene copolymer beads as a function of divinylbenzene level.

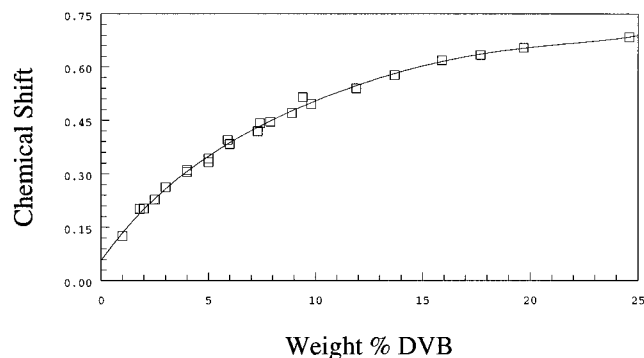


Figure 2. Dependence of the chemical shift difference (ppm) between chloroform absorbed in S-DVB copolymer beads and bulk chloroform on DVB level.

on the swelling of the copolymer by the solvent, chloroform (methylene chloride gives similar shifts). The NMR resonance of the absorbed solvent is shifted from that of bulk solvent, as shown in Figure 1. The resonance of the bulk (interstitial) solvent is used as the chemical shift reference at 7.24 ppm. The line width of this resonance broadens with decreasing levels of swelling (higher cross-linking levels) because the interstitial domain geometry and the magnitude of the susceptibility differences between bulk solvent and swollen polymer domains are a function of swelling.

The resonance of the absorbed solvent is shifted from the interstitial solvent resonance, the magnitude of the shift being directly related to the swelling of the bead. The resonance of solvent in the lightly cross-linked beads is shifted much less than that of the more highly cross-linked beads. Figure 2 gives a plot of the chemical shift difference between absorbed and interstitial chloroform as a function of the level of DVB in the copolymer. The magnitude of the shift will be shown later to be a direct function of the swelling, rather than cross-link level.

The ^1H NMR resonance from the polymer network in these systems is usually too broad to be observed, except

in the most lightly cross-linked systems. Therefore, it will be ignored in the following discussion. Important attributes for the solvents chosen include an ability to swell the network, a shift of the resonance upon absorption by the network, and a well-resolved resonance.

The origin of the shift difference, $\Delta\delta$, of the chloroform resonance observed between absorbed and interstitial chloroform for swollen S-DVB copolymers is due to the difference in the magnetic susceptibility between the internal pores of the beads relative to that of bulk chloroform outside the bead (interstitial chloroform). The aromatic rings of the styrene give rise to large ring currents which alter the magnetic environment in their vicinity.²⁸ The rings currents give rise to upfield shifts which can be larger than 1 ppm. The magnitude of the susceptibility shifts in these copolymers is a function of the mole ratio of the chloroform to the aromatic rings in the pore. The absorbed chloroform is in rapid exchange between sites within the cavity. These sites include aromatic rings and "bulk" chloroform within the cavity. The exchange is fast on the NMR time scale such that only one resonance is observed for absorbed chloroform. The more the copolymer swells, the greater the ratio of chloroform to aromatic rings within the cavity. The magnitude of the shift is dependent in this way on the swelling of the copolymer.

The resonance due to interstitial solvent is broader than that of the absorbed solvent. The broadening originates from susceptibility effects. It was possible to calculate the susceptibility broadening from the bulk susceptibilities of the two materials, and the calculated values were shown to be in good agreement with the line widths observed for the interstitial solvent.¹⁴ For solvent in a perfectly spherical environment, as with that in an idealized ion-exchange bead, the susceptibility broadening is reduced to zero. This difference in line width between interstitial and absorbed solvent is very evident from the spectra of Figure 1.

Sulfonated S-DVB Copolymers Swollen with Water. Experiments similar to those presented here were performed over 30 years ago using water as a solvent to probe the swelling of cation-exchange resins.¹⁴ The ^1H NMR resonance of the water inside the bead was shifted from that of water outside the bead for reasons analogous to those for chloroform in copolymers. In the chloroform case, the shifts were due to susceptibility effects, whereas the shifts in cation resins are due to the acidity effects of the sulfonate group. The ^1H NMR spectra of water absorbed in cation resins of different levels of swelling give a series of spectra very similar to those observed in Figure 1, except the magnitudes of the shifts are somewhat larger. The absorbed water resonance is shifted downfield (more acidic) from the bulk water outside the bead. The difference in frequency between the two resonances, $\Delta\delta$, correlates with the level of cross-linking of the sample, the shift increasing as the level of DVB in the resin increases. A plot of $\Delta\delta$ as a function of DVB level is given in Figure 3 for the series of cation standards.

Relationship between the Chemical Shift Difference, $\Delta\delta$, and Swelling. A simple model is given below which rationalizes the observed chemical shift-swelling relationship. Aromatic ring currents in the vicinity of the ring perturb the local magnetic field of the chloroform proton and shift the associated NMR resonance.²⁸ The instantaneous chemical shift of a particular probe molecule, δ_i , in a particular volume element, V_i , depends on the probe-ring proximity. Probe solvent

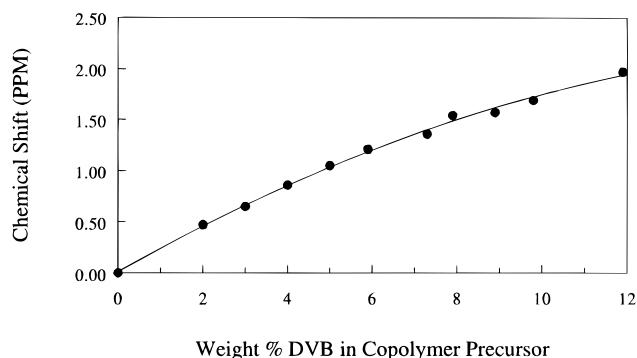


Figure 3. Effect of cross-linking on ^1H NMR shift of absorbed water for sulfonated S-DVB copolymers.

molecules undergo rapid exchange between volume elements. The observed chemical shift of a probe, δ_{obs} , is the volume-weighted average of the instantaneous local chemical shifts experienced by the probe over the time frame of the NMR experiment:

$$\delta_{\text{obs}} = \frac{\sum \delta_i V_i}{\sum V_i} \quad (1)$$

It is convenient to approximate this environment within the bead using only two distinct volume elements, a volume element with a non-zero chemical shift, V_{site} , and a volume element which is essentially not affected by the ring currents, V_{zero} . The ring current effect follows an r^{-3} probe-ring distance dependence and is limited to a small volume. All of the network samples are swollen to a significant extent (swell index between 70% and 350%) such that V_{site} is small relative to the total probe volume in the swollen network, V_{probe} ($V_{\text{probe}} = V_{\text{site}} + V_{\text{zero}}$), and V_{site} is a constant for all samples. To a first approximation, the ring-probe spatial relationships within V_{site} are a constant, independent of changes in V_{zero} , and the average chemical shift of a probe molecule in V_{site} , δ_{site} , is a constant. The observed chemical shift becomes

$$\delta_{\text{obs}} = \frac{V_{\text{site}} \delta_{\text{site}}}{V_{\text{probe}}} \quad (2)$$

where $V_{\text{site}} \delta_{\text{site}}$ is a constant for a probe-polymer series. (δ_{zero} , the chemical shift of interstitial chloroform, has been set to zero.)

In swell experiments, the total volume of the swollen system, V_{swell} , is the sum of the probe volume and the copolymer chain volume unavailable to the probe, V_0 :

$$V_{\text{swell}} = V_{\text{probe}} + V_0 \quad (3)$$

Let kV_0 be the volume of "dry" unswollen gel, where k is a constant for all S-DVB copolymers. The assumption that kV_0 is constant for all S-DVB copolymers is justified to a first approximation in that the densities of the copolymer beads are essentially equivalent, ranging from 1.04 to 1.05 g/mL. By definition, the swell index is

$$\frac{\% \text{ swell}}{100} = \frac{V_{\text{swell}} - 1}{kV_0} \quad (4)$$

Arithmetic substitution yields

$$\frac{1}{\delta_{\text{obs}}} = \frac{V_0(k-1)}{V_{\text{site}} \delta_{\text{site}}} + \frac{V_0 k}{V_{\text{site}} \delta_{\text{site}}} \left[\frac{\% \text{ swell}}{100} \right] \quad (5)$$

For a probe-polymer series, $V_0 k / V_{\text{site}} \delta_{\text{site}}$ and $V_0(k-1) / V_{\text{site}} \delta_{\text{site}}$ should be constants, and the observed chemical shift should be inversely related to the swell index.

The same phenomenology also applies to the swelling of cation resins with water, except that the shift originates from pH effects. Further, these models can be extended generally to any network system which possesses aromatic functionality which can be swollen with chloroform or acidic units which can be swollen with water. Examples of cross-linked polycarbonate and cross-linked poly(acrylic acid) will be demonstrated.

The shifts which originate from acidic functionality with water are opposite in sign to the susceptibility shifts because increased acidity gives rise to downfield shifts. S-DVB copolymer beads swollen in chloroform give rise to ^1H NMR resonances for absorbed and interstitial chloroform which are separated by as much as 0.6 ppm. These shifts are about half the size of those observed for the cation resins (pH shifts) but are surprisingly large considering that pH shifts can be an order of magnitude larger than susceptibility shifts.

Intraparticle Cross-Linking Distributions. A significant feature of this technique is its ability to determine cross-linking distributions in heterogeneously cross-linked beads. The spatial resolution of the technique is dependent on the size of the volume sampled by a probe molecule. The root-mean-squared diffusion distance that a probe molecule will travel over the duration of the experiment can be estimated using

$$X_{\text{rms}} = (2Dt)^{1/2} \quad (6)$$

where D is the self-diffusion coefficient and t is the time frame of the NMR experiment. Blum et al.^{30,31} determined the self-diffusion coefficient of toluene, chloroform, and methylene chloride in swollen S-DVB beads to be approximately $1 \times 10^{-5} \text{ cm}^2/\text{s}$. The time frame of the NMR experiment under these experimental conditions is approximately 1 ms. The calculated distance traveled by a probe molecule in this time frame is about $1 \mu\text{m}$. Cross-linking domains must be at least $10 \mu\text{m}$ to yield a probe resonance with chemical shift characteristic of the cross-linking index of that volume and not averaged with that of contiguous volume elements of different cross-linking indexes.

Obtaining the NMR spectrum of a single bead presents a formidable challenge using conventional NMR experimental procedures. The primary difficulty is associated with unpredictable line shapes and irreproducibility of the absolute shift of the resonances. These spectral artifacts arise from distortion of the applied magnetic field at interfaces of materials with different magnetic susceptibilities.

The early NMR literature on cation-exchange resins suggested that susceptibility broadening and other susceptibility artifacts could be minimized by using magic angle spinning (MAS).⁶ Recently, ^1H MAS studies of similar compounds have extended the detection limits of this technique and reduced artifacts.³⁶ MAS effectively removes susceptibility broadening features which have an orientation dependence similar to other broadening mechanisms in the solid state. In a simple analysis, the magnitude of the orientation-dependent susceptibility broadening, $\Delta_{1/2}$, may be described by the following equation.

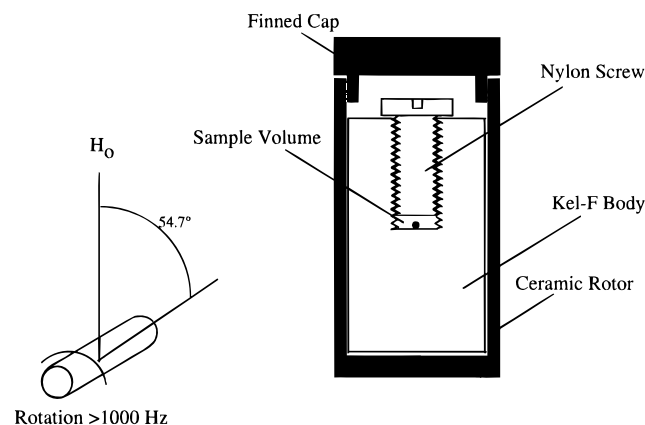


Figure 4. Schematic of the small-chamber inserts for the 4 mm ceramic MAS rotor.

$$\Delta_{1/2} = C(1 - 3 \cos^2 \theta)$$

In this expression, C is a constant which is related to the relative susceptibilities and dimensions of the materials involved as well as the applied magnetic field strength, and θ is the angle between the applied magnetic field and the susceptibility orientation of the sample. If the sample is oriented at 54.7° with respect to the applied magnetic field (the magic angle) and rotated at a frequency greater than the susceptibility broadening, then that line-broadening component is essentially eliminated from the spectrum.

A specialized small-scale sample chamber was designed for MAS rotors for the submillimeter samples (Figure 4). The chamber had an internal volume of about $5 \mu\text{L}$ and maintains the sample very near the center of the probe transmitter and receiver coils for maximum sensitivity and reproducibility. The well-sealed environment of the chamber also eliminates solvent evaporation problems. In addition, micromanipulation techniques have been applied in the development of a method with which to analyze the cross-linking present in the submillimeter cation-exchange resin.

^1H NMR Shift Correlations with Swelling for S-DVB Copolymers. Figure 1 shows the ^1H NMR spectra of a series of S-DVB copolymers of varying cross-link levels swollen with chloroform. Two resonances are observed, one due to the interstitial chloroform and the other due to the chloroform inside the bead. The magnitude of the shift between the resonances increases with increasing cross-linking. A plot of chemical shift between the two chloroform lines, $\Delta\delta$, and the level of DVB in the copolymer is given in Figure 2. (Table 3 contains the numerical values.) The sample with the largest deviation from this line is 0.2% DVB off the line. Thus, the apparent precision of the experiment to define the level of DVB within a series of copolymers made in a batch process is 0.2% absolute.

The observed chemical shift, $\Delta\delta$, should be inversely related to the swell index according to the model presented earlier and $V_0 k / V_{\text{site}} \delta_{\text{site}}$ (intercept) and $V_0 (k - 1) / V_{\text{site}} \delta_{\text{site}}$ (slope) should be constants. Figure 5 gives the plot of $1/\delta_{\text{obs}}$ as a function of % swell and shows a linear dependence with an intercept of 0.907 or $(1.10 \text{ ppm})^{-1}$. The limiting chemical shift of chloroform in toluene was 1.15 ppm (see Figure 6), in excellent agreement with this value. Thus, this simple model based on the swelling of the copolymer by the solvent and its rapid exchange within the cavity is sufficient to rationalize all of the observable NMR parameters.

Table 3. Chemical Shift Difference between Chloroform inside and outside the Bead as a Function of DVB Level in the Copolymer

sample	weight fraction of DVB	chemical shift (ppm) 30 °C	1/shift (ppm) 30 °C	$(V_e/V_0) - 1$ toluene 25 °C	$(V_e/V_0) - 1$ chloroform 25 °C	line width (ppm) 30 °C
S2	0.0197	0.2024	4.941	2.10	2.14	0.0240
S3	0.0300	0.2629	3.8037	1.80	1.79	0.0257
S4	0.0396	0.3045	3.2841	1.25	1.44	0.0227
S5	0.0497	0.3427	2.9180	1.01	1.21	0.0240
S6	0.0591	0.3946	2.5342	0.90	1.11	0.0217
S7	0.0729	0.4188	2.3878	0.73	0.92	0.0333
S8	0.0789	0.4455	2.2447	0.80	0.80	0.0340
S9	0.0886	0.4710	2.1231	0.61	0.86	0.0350
S10	0.0984	0.4916	2.0342	0.58	0.71	0.0403
S12	0.1191	0.5403	1.8508	0.69	0.60	0.0400
S14	0.1373	0.5769	1.7334	0.45	0.48	0.0616
S16	0.1591	0.6192	1.6150	0.31	0.40	0.0736
S18	0.1767	0.6344	1.5763	0.34	0.40	0.1006
S20	0.1972	0.6544	1.5281	0.26	0.30	0.1383
S25	0.2458	0.6854	1.4590	0.24	0.30	0.2292
A1	0.0100	0.1250	6.8966	3.50		
A2	0.0180	0.2010	4.9751	2.70		
A3	0.0250	0.2280	4.3860	2.10		
A4	0.0400	0.3110	3.2154	1.44		
A5	0.0500	0.3330	3.0030	1.20		
A6	0.0600	0.3830	2.6110	0.96		
A7	0.0740	0.4410	2.2676	0.80		
A9	0.0940	0.5150	1.9417	0.70		
B1	0.0600	0.4000	2.5000	1.060		
B2	0.0600	0.3100	3.2258	1.100		
B3	0.0600	0.3800	2.6316	1.060		
B4	0.0600	0.3800	2.6316	0.920		
B5	0.0600	0.2700	3.7037	1.420		
2 σ (est)	0.0002	0.008		0.08	0.08	0.009

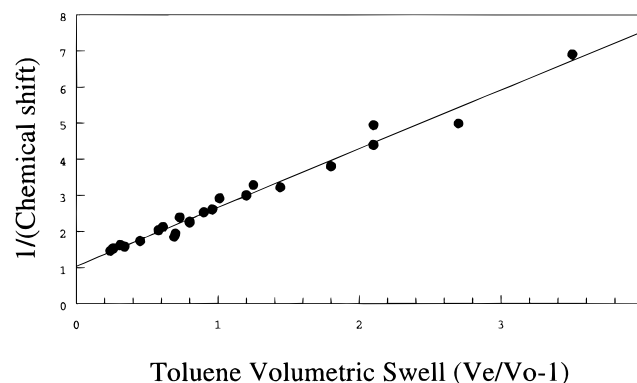


Figure 5. Dependence of the inverse chemical shift difference (ppm) between chloroform absorbed in S-DVB copolymer beads (DVB levels between 1 and 25%) and bulk chloroform on the toluene swelling.

Carbon-13 NMR is surprisingly insensitive to this effect. For example, the ^{13}C NMR spectrum of the chloroform-swollen 6% DVB copolymer did not show the same magnitude of susceptibility shift for solvent inside and outside the copolymer, as was observed in the ^1H NMR spectrum. A shoulder on the upfield side of the resonance was observed, but it was shifted only about 6 Hz (0.08 ppm). This shift was almost 1 order of magnitude smaller than that observed in the ^1H NMR spectrum. The susceptibility effects are not as pronounced for the ^{13}C nuclei because the carbon nucleus of chloroform cannot get as close to the aromatic ring as can the proton, and the ring currents have a distance dependence of r^{-3} .²⁸

Other solvents were also used as probes to gain more insight into the origin of the phenomenon. A 6% DVB copolymer was used for this experiment. Only methylene chloride gave rise to magnitudes of shifts similar

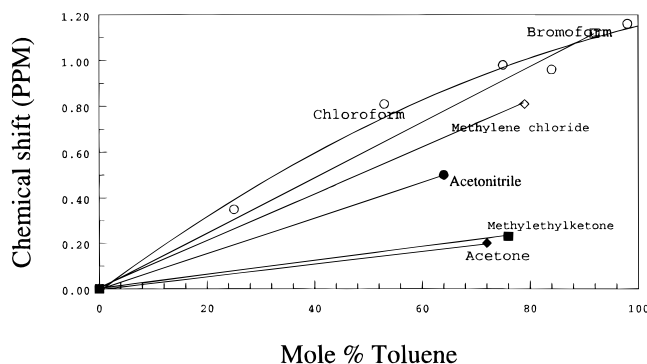


Figure 6. Dependence of the chemical shift (ppm) of various solvents on concentration in toluene.

to those observed for chloroform. The resonances of other solvents were broadened greatly, but did not show the same type of behavior as chloroform and methylene chloride. Bromoform gave very broad lines which appeared to have the same magnitude of splitting as chloroform. However, since the lines were so broad, they were not resolved.

The susceptibility shifts arise from the interaction of the proton nucleus of chloroform and the π electrons of the aromatic system. In an attempt to rationalize the relative magnitude of the shifts from one solvent to the next, the susceptibility shifts for each solvent were determined in toluene (Figure 6). The same trends exist for the susceptibility shifts in toluene that were observed for the swollen copolymers. Chloroform and bromoform have the greatest shift followed by methylene chloride, acetonitrile, methyl ethyl ketone, and acetone. The magnitude of the shifts can be rationalized in terms of the strength of the interaction between the proton of these solvents and the aromatic ring of toluene.

Precision. Experiments to define the precision of the measurement were performed on S-DVB samples synthesized with 2%, 12%, and 25% DVB. For all three DVB levels the value of the relative chloroform shift could be assigned to an estimated absolute precision of ± 2.6 Hz (0.008 ppm) at 2σ for a single measurement. Measurements of the shift at this level of precision did not require highly refined shimming or exact spectral phasing.

The precision of measuring the absorbed chloroform resonance line width ($\Delta_{1/2}$) was quite sensitive to the magnetic field uniformity and the quality of the spectral phasing. (The line width is defined as the full width at half-height.) In addition, it was found that the precision to which $\Delta_{1/2}$ may be measured is dependent on the DVB level of the copolymer. Using well-shimmed fields, the absolute precision of $\Delta_{1/2}$ for 2%, 12%, and 25% DVB was estimated to be ± 2.2 Hz (0.007 ppm), ± 4.4 Hz (0.014 ppm), and ± 5.6 Hz (0.019 ppm), respectively, at 2σ for a single measurement.

Molecular Dynamics of Chloroform in the Swollen Copolymer. The line widths of the resonances of the chloroform inside the beads also contain useful information about the environment within the microscopic cavities of the beads. Figure 1 shows that the ^1H NMR line widths of both the absorbed and interstitial chloroform resonance increase with increasing DVB level in the copolymer. The line width of the solvent outside the bead is broadened by magnetic susceptibility artifacts. These do not contribute substantially to the line shape of the resonance of the solvent inside the bead because the chloroform is within a matrix of spherical

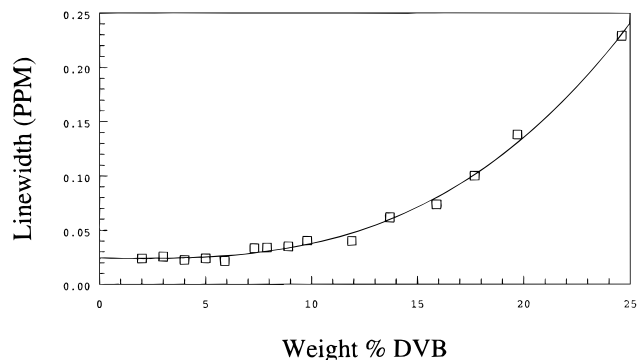


Figure 7. ^1H NMR line widths of chloroform absorbed in S-DVB copolymers as a function of the DVB level.

geometry which minimizes susceptibility broadening.²⁸ The line shape of the resonance of the solvent inside the bead is dependent on the level of swelling, the distribution of swelling within the bead, and the ability of the solvent to diffuse within the bead on the NMR time scale, which is given by the chemical shift difference between the sites in the absence of exchange (about 250 Hz). Figure 7 shows a plot of the ^1H NMR line widths as a function of the DVB level in the copolymer, and the data are listed in Table 3. The line widths remain fairly constant at 5–10 Hz between 2 and 10% DVB. At values above 10% DVB the line widths increase dramatically. The T_g values for chloroform-swollen beads were previously determined,³² indicating that at the NMR analysis temperature the beads are rubbery only for copolymers with DVB levels below about 14%. Therefore, the dynamics of the solvent molecules absorbed in the copolymers would be expected to be markedly reduced for the glassy systems relative to the rubbery copolymers. It is a well-known phenomenon that the line widths of polymers increase dramatically as the temperature is decreased below T_g .^{33,34} There are two potential origins for this broadening, both of which involve the mobility of the solvent within the bead: (1) the molecular tumbling of the solvent is restricted at higher DVB levels, or (2) diffusion of the chloroform within the bead is restricted.

The diffusion effect would cause broadening because the cross-linking distribution within a bead is inherently heterogeneous due to the differences in reactivity of styrene and the various isomers of DVB. This heterogeneity does not manifest itself as large phase-separated domains of different DVB levels within the bead, rather as heterogeneities of submicron dimensions. Since the diffusion of chloroform in lightly cross-linked copolymers is such that each chloroform molecule samples a volume of roughly $20\ \mu\text{m}$ in diameter during an NMR measurement, its resonance is not broadened by this microscopic heterogeneity. However, the diffusion rate may be slowed appreciably due to the substantially lower swelling of the higher cross-linked copolymers. Motion of the solvent throughout the copolymer matrix would thus be highly restricted. This may occur to such an extent that the rate at which a solvent probe molecule samples different cross-linking sites or environments within a bead may approach the frequency of the NMR experiment. If this happens, the chloroform ^1H NMR resonance will be broadened by an effect referred to as exchange broadening.

If the broadening is due to exchange effects, then obtaining the spectra at a much higher frequency would be expected to cause a marked change in the line width.²⁸ The line shape equation which describes these

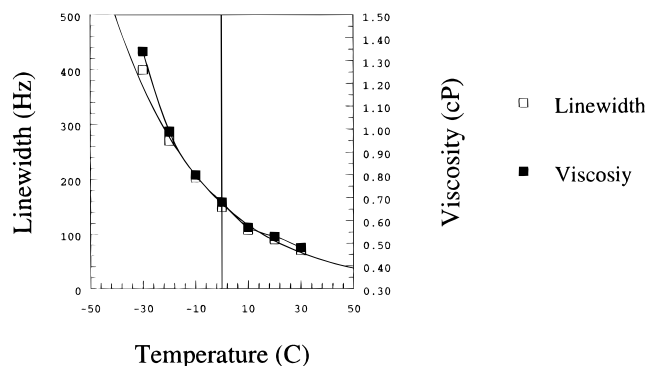


Figure 8. 300 MHz ^1H NMR line width of the absorbed chloroform in a 25% DVB copolymer and the viscosity of chloroform as a function temperature.

processes is proportional to the square of the frequency difference of the sites. For example, the line widths of spectra taken at 300 MHz would be expected to be a factor of 4 times narrower than those taken at 600 MHz if the broadening were due to exchange effects. Spectra of the 25% DVB copolymer were taken at these two field strengths, giving ^1H NMR line widths of 76 Hz at 300 MHz and 96 Hz at 600 MHz. The difference in line width is much less than the factor of 4 difference predicted from the theoretical equations of exchange broadening. It may be concluded, therefore, that exchange broadening does not contribute significantly to the chloroform ^1H NMR line widths in this 25% DVB copolymer.

The effect of temperature on the ^1H NMR line width of chloroform in the 25% DVB copolymer was also investigated. Figure 8 shows the line width as a function of temperature in the range 233–303 K. The 25% DVB sample resonance has a $\Delta_{1/2}$ value of approximately 70 Hz at 303 K which increases to 400 Hz at 233 K. The chloroform line width has a nonlinear and inverse dependence on temperature. This line broadening may be correlated with the temperature-dependent molecular motion of chloroform. The temperature-dependent molecular motions of the solvent may be examined by considering the chloroform viscosity in this temperature range. From the Stokes–Einstein equation the molecular diffusion rate has been shown to be inversely related to the solution viscosity.

The temperature-dependent chloroform viscosity is also plotted in Figure 8. As can be seen, the ^1H NMR line width of chloroform in the 25% DVB copolymer is strongly correlated with the solvent viscosity in this temperature range. This suggests that broadening of the chloroform ^1H NMR resonance may be related to restriction of molecular tumbling of chloroform in the copolymer matrix. The reduction of molecular motions of chloroform in a highly cross-linked DVB matrix may be comparable to the reduction of molecular motion of (bulk) chloroform as temperature decreases (which is manifested as an increase in bulk viscosity).

If the line width is determined primarily by lifetime broadening, then the spin–spin relaxation time, T_2 , can be determined from the line widths of the resonances as described in the expression below:

$$T_2 = (\pi\Delta_{1/2})^{-1} \quad (7)$$

A plot of the T_1 and T_2 values for chloroform inside the beads determined from its line width is shown in Figure 9 for the samples of this study. The T_2 values decrease monotonically as the DVB level in the copolymer

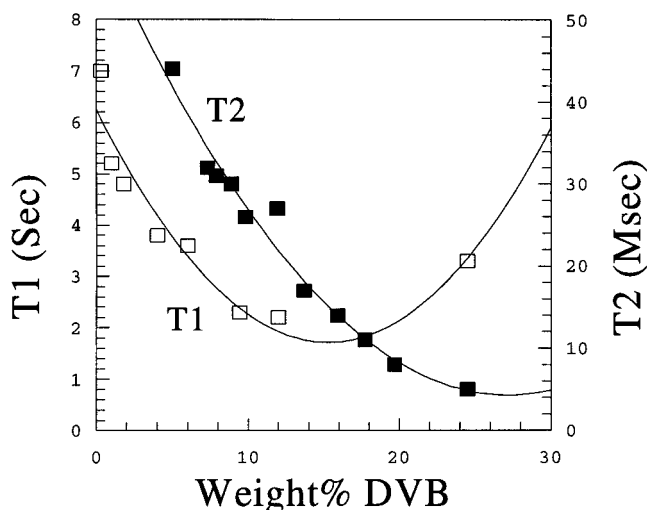


Figure 9. Dependence of ^1H NMR T_1 and T_2 of the absorbed chloroform as a function of weight percent DVB in the S–DVB copolymer measured at 300 MHz.

increases. The T_1 values decrease with increasing DVB level and actually go through a minimum, whereas the T_2 values continue to decrease with increasing DVB level. This classical NMR relaxation behavior can be explained by molecular tumbling of the chloroform being more restricted in copolymers with high levels of cross-linking.

The actual spin–spin relaxation time, was measured for the 15.9 and 24.6% DVB copolymers using the CPMG pulse sequence. These values were compared to the T_2 values determined from their line widths. The T_2 values measured using the CPMG method were 15.9 and 7.3 ms, respectively, for the 15.9 and 24.6% DVB copolymers, whereas the T_2 values measured from line widths were 11.1 and 4.1 ms. Although these values are not identical, they are similar enough to indicate that the broadening is due primarily to molecular tumbling effects. Other contributions to the line width are those of susceptibility broadening and field inhomogeneity.

The restriction in motion of the chloroform at higher cross-linking levels is an interesting observation because it reveals information about the nature of the cavities inside the copolymer bead. At low cross-linking levels, molecular tumbling is rapid, as in a bulk liquid. Above about 10% DVB, the tumbling of chloroform within the copolymer becomes restricted, suggesting that the cavity dimensions have decreased to near molecular dimensions. At still higher DVB compositions the effect is further amplified.

The volume or population fraction of bulk chloroform within a swollen cavity interacting with a benzene ring can be determined from the chemical shift of the chloroform resonance inside the bead. The site population fraction represents the volume fraction of chloroform molecules associated with an aromatic site relative to the entire chloroform population within the copolymer pores. The site population value is averaged over the lifetime of the NMR experiment. A plot of the line width as a function of the site population fraction is given in Figure 10. The line width of the chloroform inside the bead increases nonlinearly when the population fraction of chloroform at a site is greater than 0.5, or stated differently, when the number of aromatic rings is greater than the level of chloroform inside the bead. This apparently happens when the cavities inside the bead

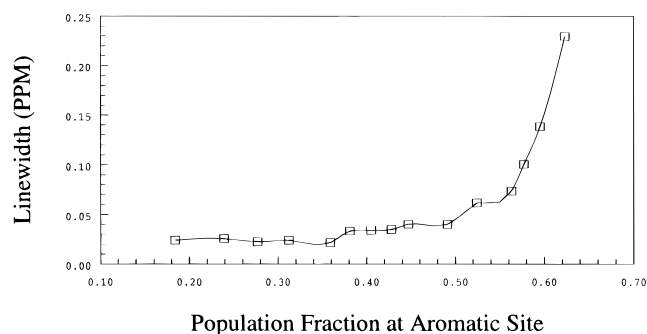


Figure 10. ^1H NMR line width of the absorbed chloroform as a function of the population fraction of chloroform interacting with a benzene ring within the cavities of the S-DVB bead.

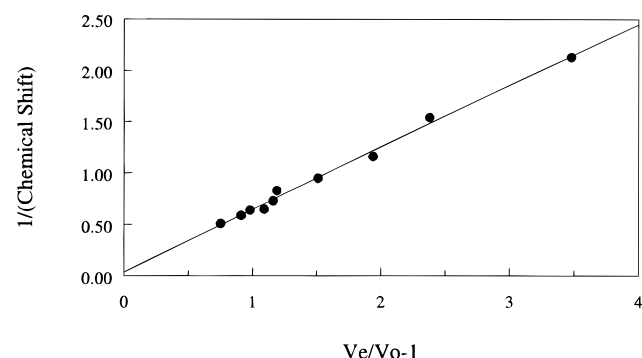


Figure 11. Effect of swelling on the inverse of the ^1H NMR chemical shift ($1/\Delta\delta$) of absorbed water for cation-exchange resins.

Table 4. Effect of Cross-Linking on Swelling of Cation Resins and the ^1H NMR Shift of Absorbed Water

wt % DVB	$\Delta\delta$ (ppm)	$1/\Delta\delta$ (ppm)	$(V_e/V_o) - 1$	line width (ppm)
2.0	0.47	2.13	3.48	0.08
3.0	0.65	1.54	2.38	0.09
4.0	0.86	1.16	1.94	0.10
5.0	1.05	0.95	1.51	0.19
	1.21	0.83	1.19	0.18
7.3	1.36	0.73	1.16	0.11
7.9	1.54	0.65	1.09	0.14
8.9	1.57	0.64	0.98	0.09
9.8	1.69	0.59	0.91	0.09
11.9	1.97	0.51	0.75	0.13

are no larger than 2 or 3 times the dimensions of the chloroform molecule itself, which has a diameter of approximately 6.5 Å. In such small cavity domains, the position or motion of one chloroform molecule may have to be correlated with neighboring solvent and matrix molecules within the cavity. Correlated motion would be increasingly difficult as the cavity dimensions decrease (with increasing cross-linking). If the swollen polymer matrix is, in fact, in a partially glassy state at high DVB levels, the correlation of solvent molecular motion with the matrix motion would lead to greatly restricted solvent molecular tumbling.

Sulfonated S-DVB Copolymers. The swelling of the beads was determined from their dry weight capacity (DWC) using the following equation:

$$\frac{V_e}{V_o} - 1 = \left(\frac{100}{\text{DWC}} - 1 \right)^{-1}$$

A plot of $1/\Delta\delta$ as a function of the swell, $(V_e/V_o) - 1$, is given in Figure 11 for the samples of this study, and the raw data are given in Table 4. The plot is, indeed, linear as expected. The value of the intercept, $0.044 \pm$

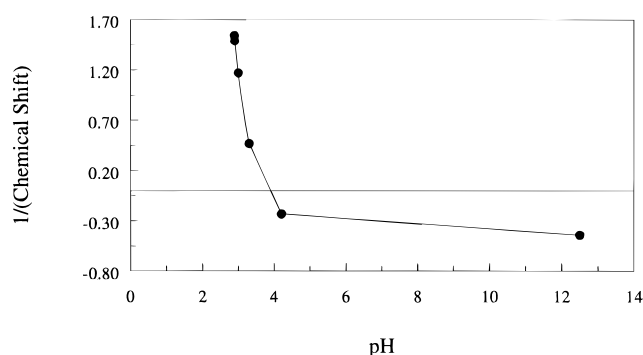


Figure 12. pH Dependence of $\Delta\delta$ (ppm) for cation-exchange resins.

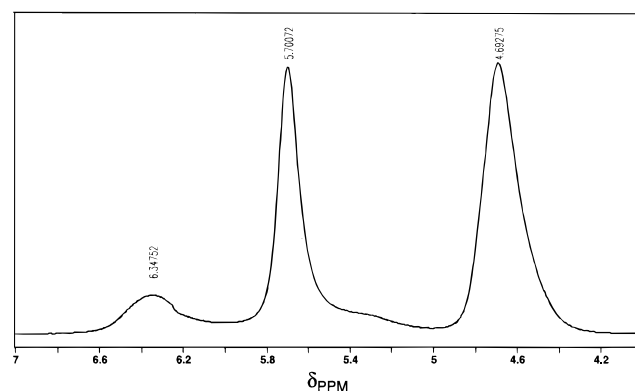


Figure 13. ^1H NMR resonances of water absorbed in a large population of cation-exchange beads obtained by high-resolution NMR.

0.06, can be used to calculate the chemical shift of a water proton at the sulfonate site according to the model. The value calculated thus is 23 ± 4 ppm downfield from the shift of the bulk water. The shifts of acidic protons in these types of sites are normally located at about 12–15 ppm, a value nearly within the precision of the fit. The precision of the $\Delta\delta$ measurement is about 0.02 ppm, smaller than the size of the circles on the plot of Figure 11. However, the precision of the swelling measurement is about twice that of the NMR measurement. Another source of error is the difficulty of sulfonating the resins uniformly, especially at high cross-linking levels.

The pH dependence of the chemical shifts of these systems was determined by measuring the ^1H NMR spectra of the 8% DVB copolymer as a function of NaOH addition. The pH was determined with a calibrated pH meter after equilibration and then the ^1H NMR spectrum was determined. The pH dependence of $\Delta\delta$ (ppm) is given in Figure 12. This figure emphasizes the need to determine $\Delta\delta$ on the resins in the acid form because the NMR measurement is strongly dependent on pH (the form of the resin). Care was taken to ensure that the resins of this study were completely converted.

Single Bead Analysis. The ^1H NMR analysis of a bulk sample of the cation-exchange resin is shown in Figure 13. It is estimated that several hundred beads are in the NMR detector volume making the analysis very representative of the entire bead population. The chemical shift scale is calibrated by assigning the maximum of the resonance associated with the interstitial or nonabsorbed water a value of 4.7 ppm. From the spectral region associated with internal (absorbed) water displayed in Figure 13, it is clear that more than one resonance is present. A main resonance is observed

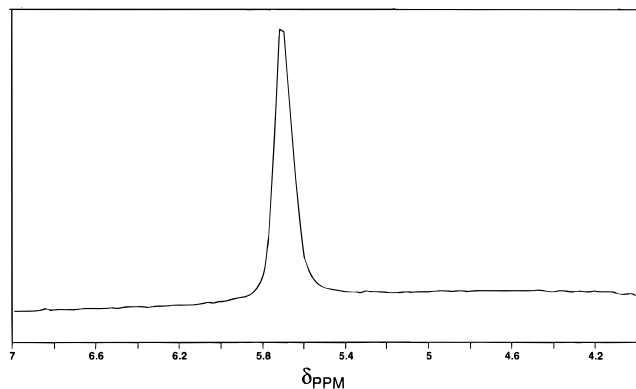


Figure 14. ^1H NMR spectrum of water absorbed in a single cation-exchange bead obtained with magic angle spinning.

at 5.70 ppm in addition to a broad resonance upfield which has one component with a maximum at approximately 6.35 ppm. There may also be a third resonance at 5.30 ppm. For this discussion we will assume that the primary influence on the relative chemical shift associated with absorbed water is the extent of cross-linking present in the bead, since the sulfonation is expected to be uniform. Therefore, there are apparently multiple cross-linking domains present in the sample. However, it is not clear from multibead experiments if the beads possess structured morphology or if the sample is a mixture of homogeneous beads with different levels of cross-linking. This differentiation requires the NMR analysis of a single bead.

The technical difficulty of performing a single-bead NMR analysis of the resin is a consequence of the very small dimensions involved. With a diameter of about 300 μm , a single bead is barely visible to the unaided eye, which makes handling and transferring individual beads very challenging. The volume of water imbibed in a fully swollen bead is only about 3 nL (based on the measured dimensions of the dried and wet beads), which corresponds to only about 150 nmol of water. In addition, because of the high surface-area-to-volume ratio of the beads, dehydration is quite rapid in ambient air.

Beads were transferred by use of a microliter-syringe needle. Individual beads could be captured in a microdroplet of water on the needle tip and transported into (or out of) the sample well of the MAS insert. When beads were placed in the rotor insert, an extra 200 nL of water was added to the chamber in before sealing with the 1-72 screw. The excess water ensured that the bead would not be dehydrated and remain completely swollen during the NMR analysis. Spectra from approximately 100 pulses were accumulated.

The ^1H NMR spectrum of a single cation bead from the sample of Figure 13, taken under the MAS conditions described above, is given in Figure 14. This spectrum shows only one resonance for water absorbed in the bead. Clearly, this bead swells uniformly throughout. (The resonance for interstitial water is sometimes not observed in these experiments because it is spun out of the detected region of the rotor.)

Figure 15 gives the ^1H NMR spectrum of a second (single) bead from this sample. This spectrum shows at least two different maxima in the resonance, indicating a swelling distribution within the bead. One maximum is located at 6.35 ppm (domain A) and the other at about 5.4 ppm (domain B). The farthest downfield resonance, that of domain A at 6.35 ppm, is the more highly cross-linked domain within the bead

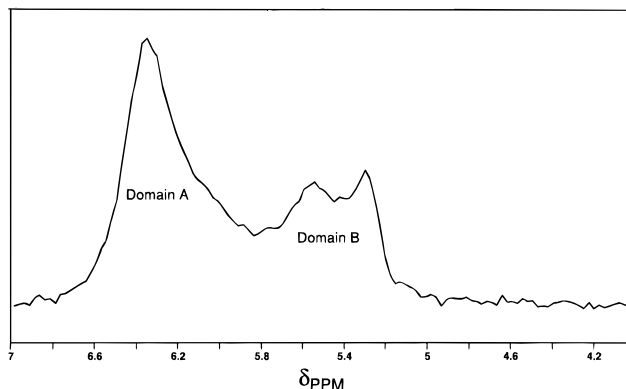


Figure 15. ^1H NMR spectrum of water absorbed in another single cation-exchange bead with magic angle spinning.

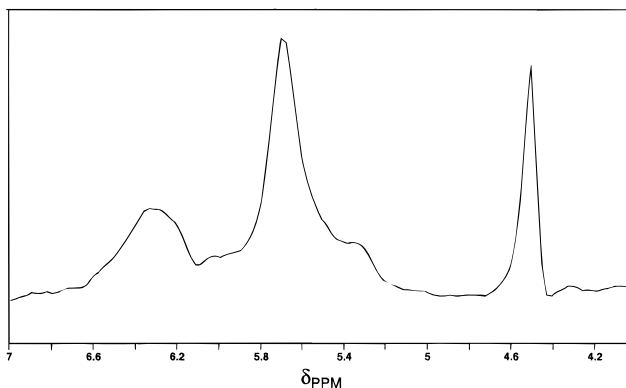


Figure 16. ^1H NMR spectrum of water absorbed in the two cation-exchange beads from Figures 15 and 16 obtained with magic angle spinning.

Table 5. Characteristics of the Bead of Figure 15 As Determined from the ^1H NMR Single Bead Measurement

domain	δ (ppm)	area	$(V_e/V_0) - 1$	weight ratio
A	6.35	2.0	0.9	80
B	5.4	1.0	2.2	20

and is also most intense, indicating that it is the larger of the domains. The relative ratios of the areas of the resonances give the relative level of water in both domains. Since the chemical shift of the resonance is correlated directly to the level of swelling of each domain by the plot of Figure 11, it is possible to define the level of swelling of each domain and to estimate their relative weight fraction of the copolymer that composes each domain. These data are given in Table 5. Domain A (the more highly cross-linked domain) represents about 80% of the copolymer within the bead and domain B, about 20%.

The two beads from Figures 14 and 15 were placed in the rotor together and the spectrum of Figure 16 was obtained. This composite spectrum is very similar to that of Figure 13, the high-resolution, multibead ^1H NMR experiment. Roughly 20 single beads were analyzed, each of which clearly fell into one of the two types of beads. Therefore, the sample is composed of a mixture of two types of beads, one of homogeneous swelling characteristics and the other which is composed of at least two domains of different swelling characteristics within the bead. This series of experiments demonstrate the usefulness of the single-bead ^1H NMR swelling experiment to characterize the cross-linking distributions within a sample of beads.

Cross-Linked Poly(acrylic acid). The level of water within the gel (the free swell capacity) is a

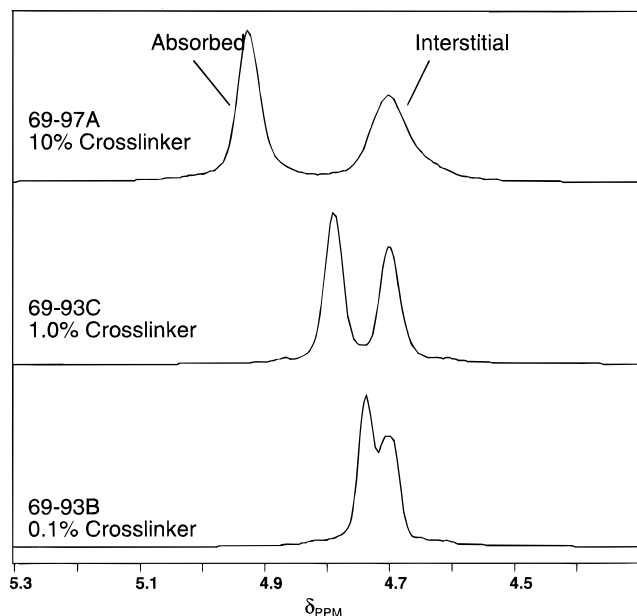


Figure 17. ^1H NMR spectra of DI water-swollen poly(acrylic acid) gel standards, acid form.

function of its swelling. The free swell capacity is defined as the weight ratio of water in the gel to poly(acrylic acid). It is related to the mole fractions of water and acid, X_w and X_a , by the following equation:

$$\text{FSC} = \frac{\text{grams}_w}{\text{grams}_{\text{PAA}}} = \frac{X_w(18)/2}{X_a(72)} = \frac{X_w(0.125)}{X_a} \quad (8)$$

where 18 and 72 are the molecular weights of water and acrylic acid, respectively. The equation which relates the free swell capacity to the ^1H NMR chemical shift difference is the following:

$$\frac{1}{\Delta\delta} = \frac{\text{FSC}}{0.125\delta_a} + \frac{1}{\delta_a} \quad (9)$$

The polymers were completely converted to the acid form as described in the Experimental Section prior to analysis because the shift differences observed for water absorbed by the polymer versus bulk water outside the bead were due to acid/base phenomena. Samples which were not converted from the salt form showed no shift between absorbed and bulk water. Therefore, it was imperative that the polymer be converted completely to the acid form in order to observe a consistent shift difference between absorbed water and bulk water. The ^1H NMR spectra of standard PAA materials made as homogeneous in cross-linker as possible are given in Figure 17. (The synthesis of these materials is also given in the Experimental Section.) The shift difference between absorbed and bulk water, $\Delta\delta$, increases as the level of cross-linking increases, as expected from the model presented earlier. A plot of $1/\Delta\delta$ versus the free swell capacity is given in Figure 18 for these three standard samples, giving a straight line, as expected, with a slope of 1.03. The value of δ_a , the shift of a proton at the acid site of poly(acrylic acid) in the absence of exchange, obtained from the slope of this line is 12.5 ppm (referenced to bulk water at 4.7 ppm). This shift is reasonable for a proton at the acid site.

The acid-form gels were also swollen in 0.9% and 10% aqueous NaCl because the gels swell less in salt solution than in DI water. Therefore, the shifts, $\Delta\delta$, were

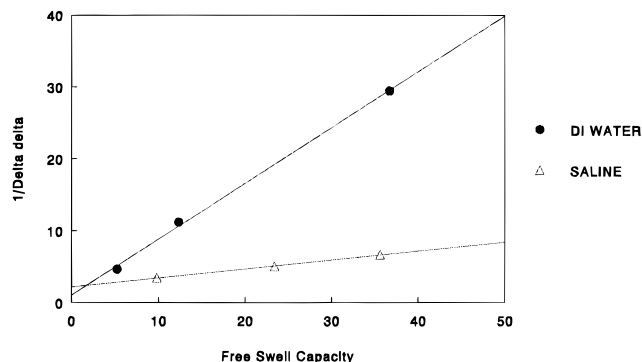


Figure 18. Dependence of $1/\Delta\delta$ on free swell capacity for poly(acrylic acid) networks.

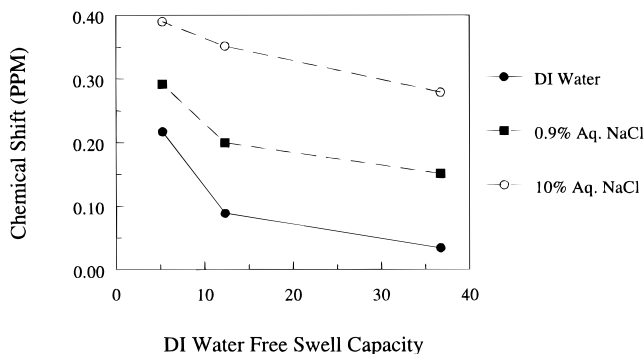


Figure 19. ^1H NMR chemical shift difference of absorbed water relative to bulk water ($\Delta\delta$) for cross-linked acrylic acid polymers swollen in water as a function of salt concentration.

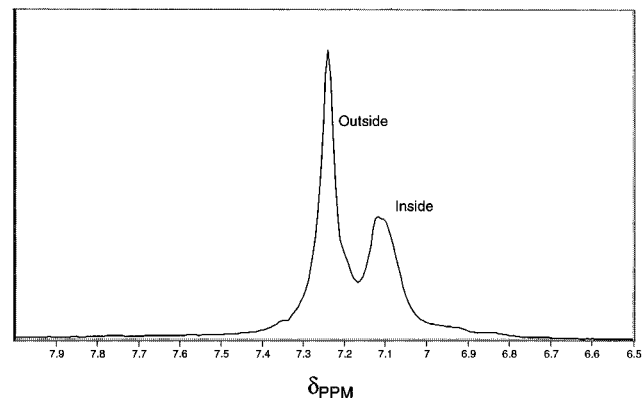


Figure 20. ^1H NMR spectrum of the 0.03 mol/mol BCB-PC sample, swollen in chloroform, 1.6 kHz.

expected to be larger in salt solution because the level of absorbed water inside the gels would decrease. A plot of $\Delta\delta$ versus the free swell capacity in DI water is given in Figure 19. As expected, the absolute values of $\Delta\delta$ are larger for the gels swollen in salt solution. However, the magnitude of the shift difference between samples of different cross-linking level actually decreases. Another way of saying this is that the slope of the plot of Figure 19 is larger for the DI water-swollen gels than for the saline-swollen gels. This results because the sodium ion competes with the protons for the acid sites in the gel, reducing the limiting chemical shift of a proton at the acid site from the value of 12.5 ppm with DI water. Therefore, the resolution of the ^1H NMR method increases with an increasing slope of this plot.

Cross-Linked Polycarbonate. A typical ^1H NMR spectrum, taken with MAS, of a swollen BCB-PC polymer is given in Figure 20. Two chloroform resonances are observed due to solvent outside the sample

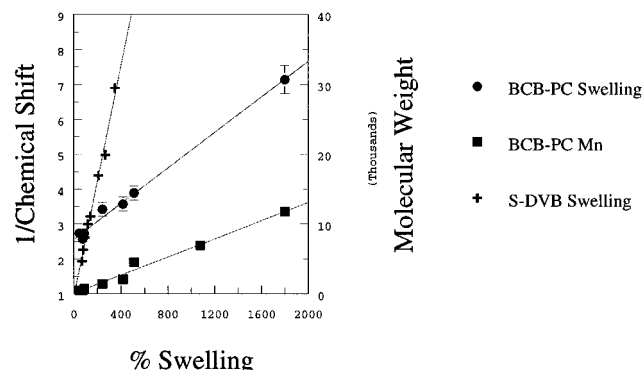


Figure 21. Correlation of the inverse of the shift difference between chloroform inside and outside for BCB-PC and S-DVB (left axis) and number average molecular weights of the uncured BCB-PC (right axis) with swelling.

resonating at a different frequency from solvent absorbed in the sample. Both resonances are fairly narrow and the shift difference between them would be expected to depend on the level of swelling of the sample. A plot of the dependence of $1/\Delta\delta$ upon swelling is given in Figure 21. The expected straight line dependence is observed. The behavior of the S-DVB copolymers from a previous study is also given on this plot for comparison. Neither the limiting chemical shifts nor the slopes of the lines are equal.

A third line on the plot of Figure 21 shows the number average molecular weight (of the BCB-PC before cure) dependence on swelling. After cure, the number average molecular weight multiplied by (BCB functionality - 1) would correspond to the average molecular weight between cross-links, M_c . There is also a correlation between swelling and M_c . In fact, the slope of the line of the number average molecular weight versus the volumetric swell was very similar to that for $1/\Delta\delta$ for BCB-PC. This further supports the fact that the two phenomena are closely related.

Discussion

The ^1H NMR analysis of swelling in polymers was demonstrated for systems with aromatic functionality using chloroform as a probe molecule, S-DVB copolymers and BCB-PC copolymers, and for polymers with acidic functionality using water as a probe molecule, cation resins and cross-linked poly(acrylic acid). Therefore, this technique appears to be general in nature for polymers with either aromatic or acidic functionality. The ^1H NMR shifts were correlated to swelling using a simple model and the calibration refined by the use of well-defined calibration standards.

The topology of the cavities within the S-DVB copolymer beads was also investigated by characterizing the molecular dynamics of the chloroform within the bead. The solvent molecular motion at 30 °C was determined to be highly restricted within copolymers of greater than 10% DVB, the extent of restriction increasing with increasing DVB level. The restricted motion was observed as line broadening in the ^1H NMR resonance of chloroform within the bead. The motion which was being restricted was determined to be molecular tumbling. Therefore, more global types of motion such as exchange between cavities must have ceased on the NMR time scale in copolymers with a much lower degree of cross-linking. This observation suggests that the cavity dimensions of the copolymer must be similar to the molecular dimensions of chloroform.

The mole ratio of bulk chloroform to chloroform which is interacting with an aromatic ring within these cavities can be easily obtained from the ^1H NMR chemical shift of the absorbed chloroform. It was shown that the line broadening increased markedly as the population fraction of chloroform associated with an aromatic site exceeded the population fraction of bulk (nonassociated) chloroform within the bead. The fact that site population increased to this extent suggested that the matrix cavities were approaching molecular dimensions. The molecular tumbling information together with these data on the ratio of bulk to bound chloroform within the cavity provide strong evidence that the average cavity size decreases dramatically with the increasing level of DVB. Moreover, molecular probes such as chloroform and bromoform can potentially be used to model the cavity dimensions in these systems.

The width of the resonance at 30 °C increases rapidly as the level of DVB exceeds about 12%. These larger line widths limit the ability of chemical shift experiments to resolve different domains in highly cross-linked systems. Elevating the temperature of the system decreases the line width. Analysis at temperatures greater than 303 K may thus increase the ability to resolve different cross-linking domains in highly cross-linked systems.

Magic angle spinning ^1H NMR was shown to be very effective for the analysis of samples which are not spherical beads or for the analysis of single beads. The artifacts due to susceptibility effects were greatly reduced using MAS. The cross-linking heterogeneities which existed within a bead were determined, both the level of swelling and the volume of each domain.

There is a strong pH dependence of the NMR shift measurement for the shifts which originate from acid effects, as was observed for the cation resin. Therefore, the acid functionality (sulfonate, carboxylate, etc.) of the polymer must be converted into the acid form prior to the analysis. Moreover, as the cation resin was being neutralized, the resonance of the absorbed water shifted uniformly upfield as the pH of the resin was changed. It was concluded from this uniform shift that the neutralization of the bead occurred homogeneously throughout the bead. If the neutralization occurred in an inhomogeneous way, such as a neutralization which proceeded from shell to core, the resonance of the absorbed water would be expected to broaden dramatically and even split into distinct resonances.

Acknowledgment. The authors would like to thank M. Tegen, A. Kott, D. Armentrout, and D. Keeley for preparing samples and helpful discussions. The support of the Dow Chemical Co. is also acknowledged.

References and Notes

- (1) Flory, P. J. *J. Chem. Phys.* **1942**, *10*, 51.
- (2) Huggins, M. L. *Ann. N.Y. Acad. Sci.* **1942**, *43*, 1.
- (3) Treloar, L. R. G. *The Physics of Rubber Elasticity*, 3rd ed.; Oxford University Press: Oxford, U.K., 1973.
- (4) Flory, P. J. *Principles of Polymer Chemistry*; Cornell University Press: Ithaca, NY, 1953.
- (5) Errede, L. A.; Newmark, R. A.; Hill, J. R. *Macromolecules* **1986**, *19*, 651-654.
- (6) Doskocilova, D.; Schneider, B.; Jakes, J. *J. Magn. Reson.* **1978**, *29*, 79-90.
- (7) Ford, W. T.; Yacoub, S. A. *J. Org. Chem.* **1981**, *46*, 819-821.
- (8) Geschke, D.; Poschel, K.; Ludwigs, K. *Polym. Bull.* **1981**, *5*, 341-346.
- (9) Ford, W. T.; Balakrishnan, T. *Macromolecules* **1981**, *14*, 284-288.

- (10) Schneider, B.; Dosckocilova, D.; Dybal, J. *Polymer* **1985**, *26*, 253–258.
- (11) Geschke, D.; Poschel, K. *Colloid Polym. Sci.* **1986**, *264*, 482–487.
- (12) Ford, W. T.; Balakrishnan, T. *Polymer Characterization, Spectroscopic, Chromatographic and Physical Instrumental Methods*; Craver, C. D., Ed.; Advances in Chemistry Series, No. 203; American Chemical Society: Washington, DC, 1983; pp 475–484.
- (13) Mohanraj, S.; Ford, W. T. *Macromolecules* **1985**, *18*, 351–356.
- (14) Gordon, J. E. *J. Phys. Chem.* **1962**, *66*, 1150–1158.
- (15) Creekmore, R. W.; Reilley, C. N. *Anal. Chem.* **1970**, *42*, 570–575.
- (16) Dosckocilova, D.; Scheider, B. *Macromolecules* **1972**, *5*, 125–127.
- (17) Frankel, L. S. *Anal. Chem.* **1971**, *11*, 1506–1508.
- (18) de Villiers, J. P.; Parrish, J. R. *J. Polym. Sci., Part A* **1964**, *2*, 1331.
- (19) Smith, W. B.; Strom, E. T.; Woessner, D. E. *J. Magn. Reson.* **1982**, *46*, 172.
- (20) Creekmore, R. W.; Reilley, C. N. *Anal. Chem.* **1970**, *42*, 725.
- (21) Frankel, L. S. *J. Phys. Chem.* **1971**, *75*, 1211.
- (22) Narebska, A.; Streich, W. *Colloid Polym. J.* **1980**, *258*, 379.
- (23) Ford, W. T.; Periyasamy, M.; Spivey, H. O.; Chandler, J. P. *J. Magn. Reson.* **1985**, *63*, 298.
- (24) Periyasamy, M.; Ford, W. T. *React. Polym.* **1985**, *3*, 351.
- (25) Sternlicht, H.; Kenyon, G. L.; Packer, E. L.; Sinclair, J. J. *Am. Chem. Soc.* **1971**, *93*, 199.
- (26) Hinton, J. F.; Amis, E. S. *Chem. Rev.* **1967**, *67*, 367–425.
- (27) Ogino, K.; Sato, H. *J. Appl. Polym. Sci.* **1995**, *58*, 1015–1020.
- (28) Pople, J. A.; Schneider, W. G.; Bernstein, H. J. *High Resolution Nuclear Magnetic Resonance*; McGraw-Hill: New York, 1959; Chapter 10.
- (29) Shaw, D. *Fourier Transform NMR Spectroscopy*; Elsevier Scientific Publishing Co.: New York, 1976; Chapter 10.
- (30) Ford, W. T.; Ackerson, B. J.; Blum, F. D.; Periyasamy, M.; Pickup, S. *J. Am. Chem. Soc.* **1987**, *109*, 7276–7280.
- (31) Pickup, S.; Blum, F. D.; Ford, W. T.; Periyasamy, M. *J. Am. Chem. Soc.* **1986**, *108*, 3987–3990.
- (32) Gutierrez, M. H.; Ford, W. T. *J. Polym. Sci., Part A: Polym. Chem.* **1986**, *24*, 655–663.
- (33) Dekmezian, A.; Axelson, D. E.; Dechter, J. J.; Borah, B.; Mandelkern, L. *J. Polym. Sci., Polym. Phys. Ed.* **1985**, *23*, 367–385.
- (34) McDonald, C. J.; Smith, P. B.; Roper, J. A.; Lee, D. I.; Galloway, J. G. *Colloid Polym. Sci.* **1991**, *269*, 227–241.
- (35) Marks, M. J.; Sekinger, J. K. *Macromolecules* **1994**, *27*, 4106–4113.
- (36) Sarkar, S. K.; Garigipati, R. S.; Adams, J. L.; Kiefer, P. A. *J. Am. Chem. Soc.* **1996**, *118*, 2305–2306.

MA960650G